Concentration and binary separation of micro particles for droplet-based digital microfluidics†

Sung Kwon Cho,*[a] Yuejun Zhao[a] and Chang-Jin "CJ" Kim[b]

Received 31st October 2006, Accepted 22nd January 2007
First published as an Advance Article on the web 12th February 2007
DOI: 10.1039/b615665g

This paper describes a concept of concentration and binary separation of particles and its experimental confirmations for digital microfluidics where droplets are driven by the mechanism of electrowetting-on-dielectric (EWOD). As a fundamental separation unit, a binary separation scheme is developed, separating two different types of particles in one droplet into two droplets, one type each. The separation scheme consists of three distinctive steps, each with their own challenges: (1) isolate two different types of particles by electrophoresis into two regions inside a mother droplet, (2) physically split the mother droplet into two daughter droplets by EWOD actuation so that each type of particle is concentrated in each daughter droplet, and (3) free the daughter droplets from the separation site by EWOD to ready them for follow-up microfluidic operations. By applying a similar procedure to a droplet containing only one type of particle, two daughter droplets of different particle concentrations can be created. Using negatively charged carboxylate modified latex (CML) particles, 83% of the total particles are concentrated in a daughter droplet. Successful binary separation is also demonstrated using negatively charged CML particles and no-charge-treated polystyrene particles. Despite the undesired vortex developed inside the mother droplet, about 70% of the total CML particles are concentrated in one daughter droplet while about 70% of the total polystyrene particles are concentrated in the other daughter droplet.

1. Introduction

Much emphasis has been directed towards the development of "lab-on-a-chip"[1–7] since its concept was introduced in the early '90s.[7] To date, most of these systems have been developed based on continuous flows. Biological and chemical solutions are dispensed, pumped, mixed and regulated in a network of microchannels fabricated on a substrate (Fig. 1). The microchannel network is necessarily a core element in such a system. Pumps, valves and mixers are used for basic and advanced fluidic handling, and some components are often integrated into a single substrate with the microchannels. As a result, a complete continuous flow system tends to require complicated micromechanical structures, often raising the cost of design and fabrication and lowering the reliability of operation. Moreover, these types of systems are usually application-specific and offer little flexibility. A different approach imposing the least mechanical complication in the device and allowing reconfigurability by the users is highly desired.

Recently much attention has been drawn to the possibility of a lab-on-a-chip system run by droplet-based (digital) microfluidics.[8–19] These systems differ from continuous flow systems in that they handle fluids in the form of discrete droplets rather than continuous streams. After microactuation of fluid packets by temperature gradients in the microchannel,[20,21] Washizu[14] first demonstrated electrostatic transportation and the merging of water droplets on a substrate covered with a hydrophobic layer. More recently, dielectrophoretic forces were used to transport droplets.[15,16] Many of such microdevices have attempted to harness surface tension, for its dominance in micro scale, for micro fluid actuations.[22–24] Among several methods known to control surface tension, electrowetting, which uses electric potential to control wettability of a solid surface, is considered the most promising.[22]

The concept of digital microfluidics was proposed when droplet-based microfluidics became promising as a general fluid micromanipulation principle by electrowetting-on-dielectric or

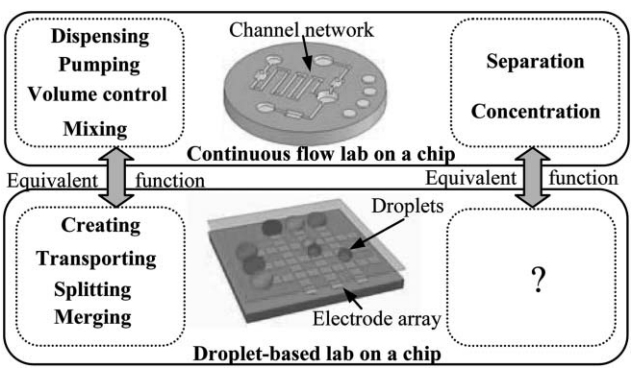

Fig. 1 Why do we need to develop separation/concentration units for droplet-based lab-on-a-chip systems?

[a]*Department of Mechanical Engineering and Materials Science, University of Pittsburgh, 3700 O'Hara St., Pittsburgh, PA 15261, USA. E-mail: skc@engr.pitt.edu; yuz21+@pitt.edu; Fax: +1 412-624-4846; Tel: +1 412-624-9798 Tel: +1 412-624-7823*
[b]*Mechanical and Aerospace Engineering Dept., University of California, Los Angeles (UCLA), 420 Westwood Plaza, Los Angeles, CA, 90095, USA. E-mail: cjkim@ucla.edu; Fax: +1 310-206-2302; Tel: +1 310- 825-0267*
† The HTML version of this article has been enhanced with colour images.

EWOD (for an extensive review on EWOD, see Mugele and Baret[25]). While microactuation by electrowetting had been proposed a while ago,[24] an operational microdevice has first been developed based on continuous electrowetting of liquid–metal droplets.[23] The manipulation of aqueous liquids needed additional findings for reversible actuation,[26] a means to lower the driving voltages,[27] and device fabrication to allow manipulation of liquids in an air environment.[8,9] This was advanced greatly after the four fundamental operations essential for digital microfluidics were successfully analyzed and experimentally obtained:[12,13] creating, transporting, splitting, and merging droplets. All of these droplet-based operations can be performed on chip by programming an electric signal rather than adding physical structures for a certain fluidic function. A similar development has been reported for the special case of two-liquid systems (*i.e.*, water droplets on a solid surface immersed in oil), where droplets slide with little resistance.[10,11]

More advances have been made to the EWOD-based microfluidics. A significant mixing enhancement can be achieved by merging two different droplets and moving the merged droplet in programmed paths with EWOD actuation.[28,29] Another important development for lab-on-a-chip applications is the EWOD operations on a full $M \times N$ grid array enabled by a novel cross-referencing scheme,[30] which requires only a single conduction layer, thereby simplifying fabrication and electrode wiring for two-dimensional array chips. More recently, two-dimensional arrays capable of direct referencing have been introduced by fabricating the EWOD chip on a multi-layer printed-circuit board (PCB).[31] This simplicity has led to a handheld digital microfluidic system,[32] an important step towards lab-on-a-chip.

Riding on all these developments, the conventional fluidic operation units in the continuous flow system such as dispensing, pumping, volume control, and mixing can be possibly achieved in many cases by the pure droplet operation units such as creating, transporting, splitting, merging, and mixing (Fig. 1). The fabrication process is simpler with no need to build moving micromechanical parts in the device. Therefore, the resulting system is simpler, more reliable, and more cost-effective for design and fabrication. Furthermore, by simply changing the activation program of the electrode array, a new microfluidic task can be performed on a given chip. This flexibility (*i.e.*, reconfigurability) allows a wide variety of applications without building a dedicated chip for each application, thus offering the capability of mass production. Compared with electrokinetic driving methods, EWOD consumes extremely low power (in μW's), an especially promising feature for portable systems.

Most recently, this EWOD technology has been extended for applications in biomedicine. For example, Srinivasan *et al.*[33] demonstrated a glucose detection process using droplet operations of merging and transporting. Wheeler *et al.*[34] reported an automated sample preparation for matrix-assisted laser desorption/ionization mass spectrometry by moving and merging droplets, including sample purification[35] and even an integrated chip for parallel processing.[36] Zhao and Cho[37,38] demonstrated that EWOD-actuated droplets can efficiently sweep and sample airborne particles on solid surfaces, facilitating a handheld airborne particle monitoring system. However, most biological assays and chemical processes require fluidic operations more sophisticated than the fundamental droplet operations (creating, transporting, splitting, and merging). One of the first and often most important tasks in biochemical processes is the concentration and/or separation of different types of bioparticles and molecules.[39] These units in continuous flow systems are often carried out by using centrifuges, capillary electrophoresis or others. The lack (Fig. 1) of counterparts in digital microfluidics would limit the scope in many practical applications of digital microfluidic lab-on-a-chip systems.

In this paper, we describe a new class of concentration and binary separation (*i.e.*, separation of two different types of particles) of micro particles for droplet-based fluidics and demonstrate the proof of concept along with performance quantifications. Concentration and binary separation processes are successfully implemented in the domain of droplets by incorporating electrophoresis inside a droplet and manipulating the droplets by EWOD actuation. In order to quantify the concentration and separation efficiency, populations of particles before and after the operations are measured, using a direct particle counting method. The concept of the present concentration and separation scheme and some preliminary results have been previously reported in ref. 40.

2. Concept

The concept of binary separation is illustrated in Fig. 2, following the first report by Cho and Kim.[40] In a droplet-based microfluidic circuit, a single mother droplet containing mixed particles (types A and B) is placed between two parallel plates (Fig. 2(a)). The separating procedure mainly consists of three steps. First, isolate each type of particle by

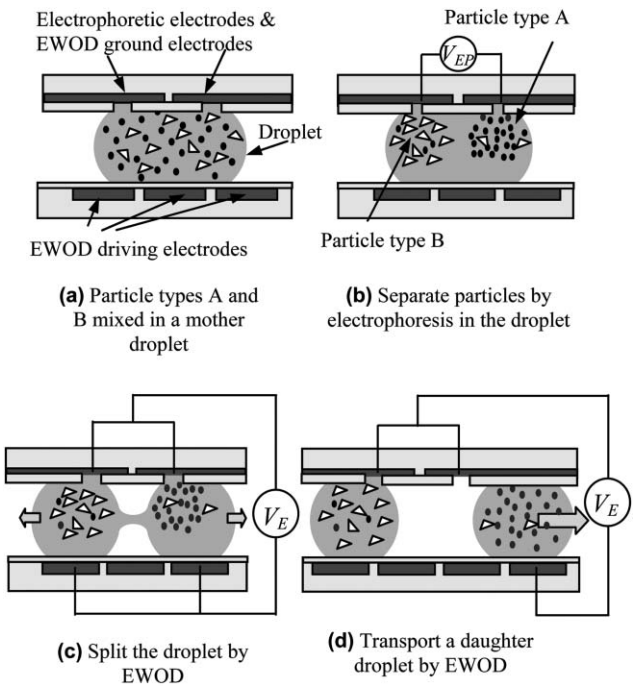

Fig. 2 Cross-sectional schematic views of particle separation in a droplet and subsequent droplet splitting and transporting.

electrophoresis within the droplet (Fig. 2(b)). The particles can be discriminated by the difference of their polarity and mobility. As a particular case, consider two types of particles with opposite polarities: one type is negatively charged and the other positively charged. Under an electric field, the negatively charged particles would be attracted to the anode and the positively charged ones to the cathode. For example, as shown in Fig. 2(b), the particles of type B (open triangles) are on the left side and the particles of type A (solid circles) on the right side in the droplet.

Second, physically split the mother droplet into two daughter droplets (Fig. 2(c)). When the electrodes beneath the two opposite ends of the droplet in Fig. 2(b) are activated, the two ends of the droplet are wetting and pulling the droplet apart while the droplet is pinched in the middle. If conditions are met, the droplet is eventually split into two daughter droplets. For the conditions of splitting, we have previously reported design rules, mechanisms and experimental verifications.[12,13] As a result, the particles of type B are more concentrated in the left daughter droplet than the right daughter droplet, and vice versa for the particles of type A (Fig. 2(d)). This step corresponds to the extraction of separated entities.

Third, free the daughter droplets from the separation electrodes and transport them to other locations, all by EWOD actuation (Fig. 2(d)), for subsequent microfluidic operations. This step involves certain challenges, described in the later section on experimental results. For a high degree of separation precision, multiple daughter droplets with the same particle type can be re-joined and the same separation procedure may be repeated, which can be naturally accommodated in digital microfluidics. Meanwhile, for the separation of multiple kinds of particles, the same principle can be used to separate and extract each particle type one by one by repeating the same procedure. Therefore, the proposed binary separation can constitute a fundamental unit for more complicated and advanced separation procedures that we envision.

The concept of concentration is similar to and simpler than the separation procedure described above. If there exists only one type of particle in a mother droplet, the electrophoretic force induces migration of the particles to a certain area. After local concentration of the particles is achieved, the splitting process is activated, thereby creating two daughter droplets having different concentrations.

This scheme provides several significant and unique advantages. First, the electrophoretic actuation in such a limited space as inside a droplet can be easily and directly interfaced to conventional electronics since it requires only additional electrodes. Second, by simply switching electric connections from electrophoretic actuation of particles within a droplet to EWOD actuation of droplets, the particles can be quickly extracted and secured in daughter droplets with minimum dispersion. Third, two fluidic operations (*i.e.*, separation and concentration) can be performed in the same device without adding any supplementary devices or electrical components.

3. Testing device fabrication

The testing devices, which mainly consist of two parallel channel plates, were fabricated using microfabrication technologies. Fig. 3 shows perspective and cross-sectional views of the testing device. The detailed fabrication steps for the EWOD channel structure were described in Cho *et al.*[13] and Moon *et al.*[27] The channel gap was fixed at 70 μm for successful droplet splitting based on the design rule.[12,13] The bottom plate has addressable driving electrodes of square type (1.4 mm × 1.4 mm) beneath dielectric layers while the electrodes for electrophoresis were located on the top glass plate. The transparent ITO layer on the top plate was split into two sections as shown in Fig. 3(b). In each electrode section, a small window (60 × 300 μm^2) was opened through the Teflon® layer to provide a direct electrical contact with the liquid droplet so that an electric field could be generated within the droplet for electrophoresis. Opening the Teflon® layer was done by the photolithography and an RIE (reactive ion etching) process in oxygen plasma. Since the Teflon layer is very hydrophobic, it is difficult to spin-coat a photoresist on the Teflon® surface for the photolithographic process. This problem could be overcome using a fluorocarbon surfactant.[41] With this photolithographic process, the hydrophobicity of the Teflon® layer remained without much degradation (less than 5° contact angle reduction).

The applied voltage V_{EP} for electrophoresis was variable but limited to below about 5 V_{DC} due to electrolysis; the electric potential V_E for EWOD actuation was set at ~60 V_{AC} (10 kHz). The fabricated devices were tested under a

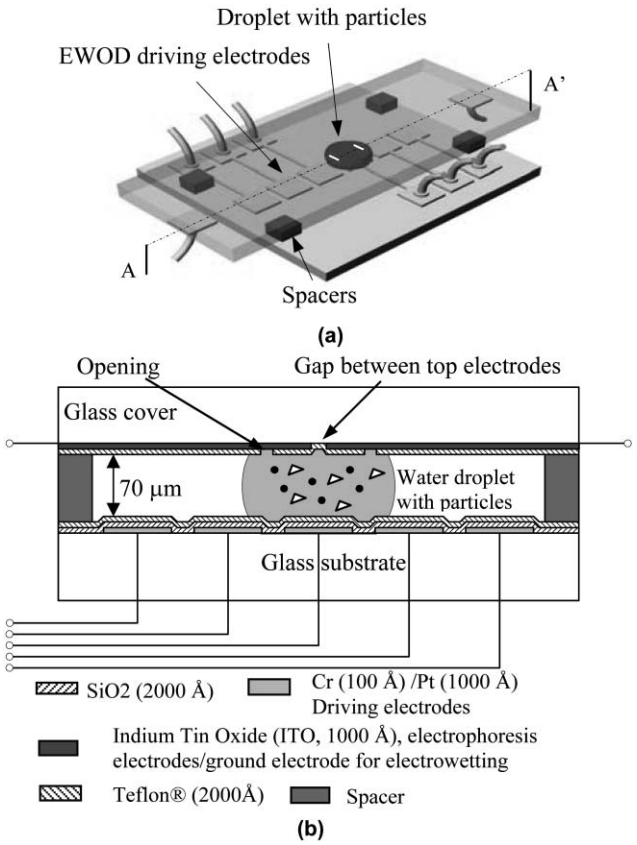

Fig. 3 Testing devices. (a) Perspective view. Note that electrodes for electrophoresis on the top glass cover are transparent, so they are invisible. Particles are not drawn for clarity; (b) View of cross-section A–A′. Not to scale.

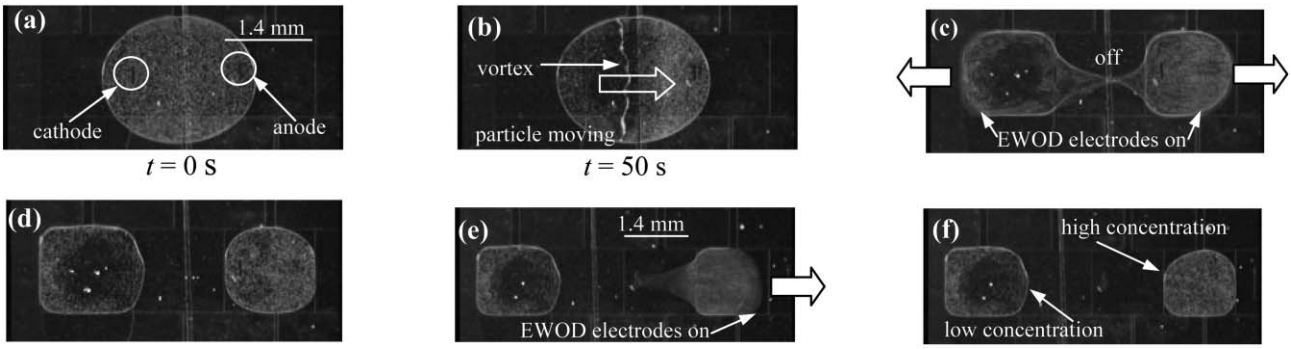

Fig. 4 Sequential images of particle concentration: (a) CML particles in a droplet; (b) electrophoresis is on. The CML particles migrate to the anode. Note that a vortex is formed and its line starts to distort in the middle of the droplet; (c) splitting of the droplet by EWOD actuation; (d) the right droplet has higher populations of the particle than the left droplet does; (e) the right droplet is transported to the right by EWOD actuation. Note that the tail of the droplet is also pinned on the anode surface for a moment; (f) completion of the whole process.

microscope using particles with and without charge treatment that were differentiable by their size and color.

4. Experimental results

4.1 Particle concentration

4.1.1 Proof-of-concept experiment. If only a single type of particle exists in a droplet, particle concentration can be controlled by electrophoresis and EWOD actuations. Fig. 4 shows experimental results for concentration control. Initially the droplet in Fig. 4(a) contains CML particles (carboxylate modified latex, 2 μm in diameter, Interfacial Dynamics Corp.) which are negatively charged on the particle surface. In preliminary experiments the mobility of the CML particles in DI water was roughly estimated to be about 1 $\mu m\ s^{-1}\ V^{-1}\ cm$. When an electric field (about 3.3 $V\ mm^{-1}$) is generated in the water droplet by applying a voltage between the two open contacts on the top plate, the CML particles are electrophoretically attracted and migrated to the anode. Note that the anode and the cathode are not clearly visible since electrodes for them are made of transparent ITO. After migration the right side of the droplet has more populations of the particle than the left side does. After about 50 s, the splitting process is in order. The left and right EWOD electrodes at the two opposite ends of the droplet are activated at $V_E = 60\ V_{AC}$ and 10 kHz with the middle electrode off such that the droplet starts to elongate and the middle of the droplet contracts. The split process itself is completed within 1/15 s. As a result, two daughter droplets are produced with different particle concentrations: low concentration in the left daughter droplet and high concentration in the right daughter droplet (Fig. 4(d)).

In the mean time, Fig. 4(e) illustrates that the split daughter droplet can be transported to other locations for follow-up fluidic processes. One concern in this step is whether or not the split droplet can be freed from the anode (or cathode) of which the surface is highly hydrophilic (ITO electrode surface). If the adhesion is stronger than the EWOD driving force, the daughter droplets would remain stuck on the split site and this concentration scheme would restrict the subsequent fluidic processes. For the anode opening area of 60 × 300 μm^2, however, detaching of the daughter droplets was successfully accomplished (Fig. 4(f)) despite a tail formed momentarily by a liquid pinning on the anode surface (Fig. 4(e)). There might remain some water residues on the anode surface, but they were not observable perhaps because of fast evaporation. This pinning brings about a design issue in determining the size of the electrode opening. For a more uniform electric field, a larger opening area may be required, which, however, would make detaching more difficult. A trade-off between the two conflicting factors is necessary in the device design.

4.1.2 Quantification of particle concentration. To accurately evaluate the concentration efficiency, the number of particles in a droplet should be counted before and after the particle concentration operation. However, since particles are generally clustered in the droplets when stagnant, it is difficult to make accurate on-chip measurements. In the present work, instead, off-chip measurements were carried out using a disposable hematocytometer (Cell-VU® CBC) and the 'touch count' function in an image analysis software tool (analySIS® FIVE). The hematocytometer is commercially available and widely used for manual cell counting. This hematocytometer provides relatively uniform particle distributions in a shallow chamber with minimal clustering so that the particles are easily differentiated and can be manually counted one by one. The hematocytometer used consisted of a chamber covered with a grid-patterned glass plate (Fig. 5). On the chamber cover plate 3 × 3 large square grids with 1 mm spacing were engraved. Each grid square had sub grids of 10 × 10 or 4 × 4 that were equally spaced. The depth of the chamber was 20 μm, giving the total chamber volume of 0.18 μl. After finishing the concentration or separation operation, each daughter droplet was sucked into a pipette and transferred to the hematocytometer chamber. If necessary, DI water was added in order to have better uniformity in the chamber or wash the chip surface for minimal particle loss in transfer. However, this added water amount was taken into account in the final particle concentration measurements. Then, micro plan images through the glass cover plate were taken (Fig. 5) so that each particle on the images was manually counted using the image software tool.

Before measuring real samples, the accuracy of this method was evaluated. First two different kinds of particles were

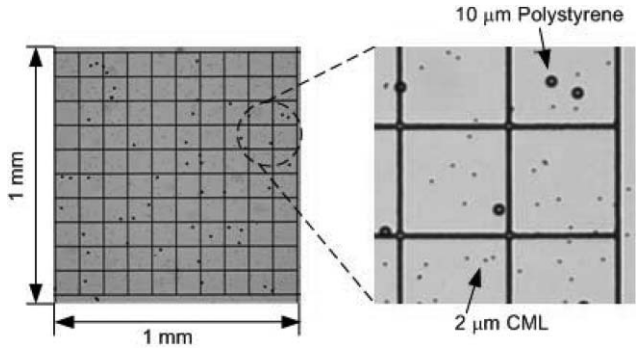

Fig. 5 Uniformly distributed mixed particles in a hematocytometer chamber. Two types of particles (CML and polystyrene) are clearly differentiable by size. The hematocytometer has 9 squares, each square (shown left) measuring 1 mm × 1 mm. Within a square, there are 10 × 10 or 4 × 4 sub grids that are equally spaced.

mixed into a 398 μl DI water solution: 2 μl CML particle solution (2 μm in diameter, 3.8% solid-to-liquid volume ratio) and 100 μl polystyrene particle solution (10 μm in diameter, 1% solid-to-liquid volume ratio, Duke Scientific Co.). The hematocytometer images of the mixed particles are shown in Fig. 5. The ratio of CML-to-polystyrene particle numbers in the mixed solution was calculated at 10.72 using the solid-to-liquid volume ratios given by the manufacturers while the hematocytometer method measured 11.64. The discrepancy between them is 8.6%, indicating the hematocytometer method is pretty accurate.

How many particles are finally concentrated in each split daughter droplet is strongly dependent on when the mother droplet is split after electrophoresis starts. Let us define cut-off time $t_{\text{cut-off}}$ as the elapsed time until the droplet splitting is activated after the electrophoresis is activated. In order to investigate the effect of the cut-off time to the final concentration in the daughter droplets, five different runs have been carried out with similar initial concentrations in the mother droplet but with different cut-off times ($t_{\text{cut-off}}$ = 20, 40, 60, 80 and 100 s). Shown in Fig. 6(a) are final split droplets of each case. In the left droplets, the number of particles decreases as $t_{\text{cut-off}}$ increases until $t_{\text{cut-off}}$ = 60 s, after which it increases again. While the particle number in the right daughter droplet is too high in all five cases to observe the trend, we can infer from the conservation of total particles that the trend is the opposite for the right droplet. The increased concentration in the left droplet after $t_{\text{cut-off}}$ = 60 s is due mainly to the vortex generation near the center of the mother droplet (Fig. 4(b)). The fluid circulates in the vortex formed near the center region, prohibiting particles from being concentrated in the right side. To maximize the concentration, the cut-off time needs to be optimized using a provision to monitor the concentration.

The above visual results are consistent with the hematocytometer particle counting results, as shown in Table 1 and Fig. 7. Since the volume of the split droplet varies, the following two quantities are considered for concentration efficiency evaluation: concentration (number of particles μl^{-1}) in each split droplet and the ratio of particle number in each split droplet to the total particle number (shown in parentheses in Table 1). Note that the maximum concentration in the right

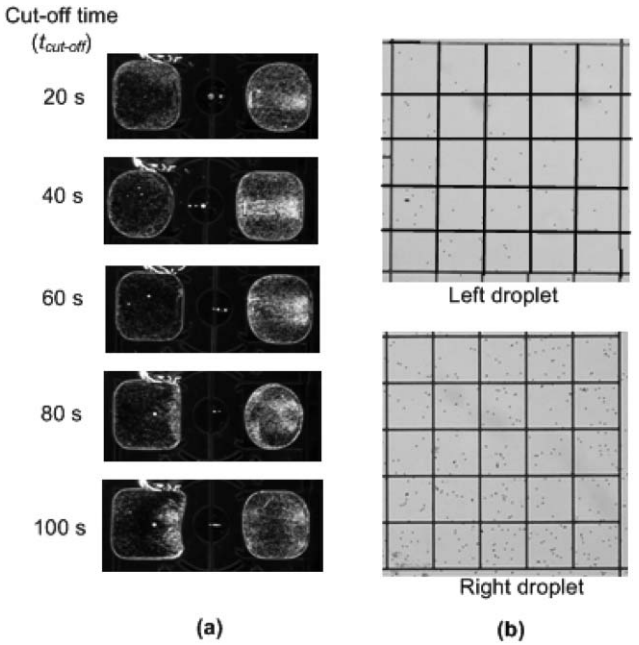

Fig. 6 Effects of the cut-off time ($t_{\text{cut-off}}$) on particle concentration. (a) The particle concentration in the left daughter droplet decreases with $t_{\text{cut-off}}$ until $t_{\text{cut-off}}$ = 60 s and increases after, and vice versa in the right daughter droplet. When $t_{\text{cut-off}} \approx 60$ s, the separation efficiency is maximum. (b) Hematocytometer particles images of split droplets at $t_{\text{cut-off}}$ = 60 s.

Table 1 CML particle concentration at different cut-off time. The numbers in parentheses represent the percentile to the total number of CML particles

	Left droplet		Right droplet	
$t_{\text{cut-off}}$/s	Volume/μl	Concentration, C_L/number of particles μl^{-1}	Volume/μl	Concentration, C_R/number of particles μl^{-1}
20	0.21	24809 (30%)	0.19	64595 (70%)
40	0.19	16689 (20%)	0.22	58995 (80%)
60	0.22	12715 (17%)	0.20	69488 (83%)
80	0.24	19629 (27%)	0.17	73944 (73%)
100	0.26	29555 (40%)	0.21	54382 (60%)

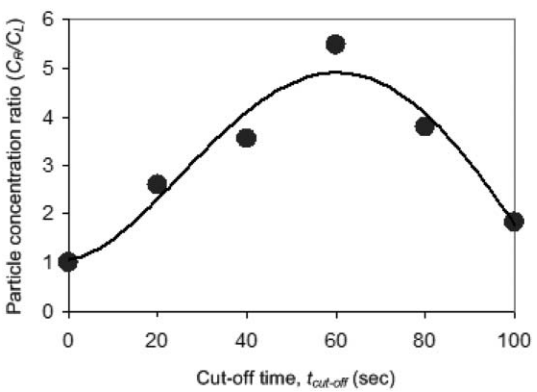

Fig. 7 Particle concentration ratio (C_R/C_L) between the right and left droplets with different cut-off time, $t_{\text{cut-off}}$. For the conditions described above, the maximum occurs at $t_{\text{cut-off}} \approx 60$ s. The data are curve-fitted by a fourth-order polynomial function.

droplet occurs at $t_{cut\text{-}off}$ = 80 s, not 60 s. However, the percentage of particles taken into the right droplet is maximum (83%) at $t_{cut\text{-}off}$ = 60 s. This is because for the case of $t_{cut\text{-}off}$ = 80 s, the volume of the right droplet is the smallest among the five cases and the total number of particles ($19629 \times 0.24 + 73944 \times 0.17 \approx 17281$) happened to be larger than the case of $t_{cut\text{-}off}$ = 60 s ($12715 \times 0.22 + 69488 \times 0.2 \approx 16576$). Based on the particle concentration ratio of the right-to-left droplets C_R/C_L, as shown in Fig. 7, the optimal cut-off time is considered to be $t_{cut\text{-}off}$ = 60 s, where the concentration ratio is maximized at 5.5 and 83% of all the particles are taken into the right droplet. The process has entailed a $\sim$70% increase in the concentration compared to the concentration of the mother droplet.

4.2 Binary particle separation

4.2.1 Proof-of-concept experiment. A similar procedure, described in Fig. 2, can be applied to separate two different types of particles. Initially two different kinds of particles are mixed in a mother droplet (Fig. 8(a)): 2 μm CML particles with a negative charge treatment on the surface (shown dark yellow in the HTML color version) and 10 μm polystyrene with no charge treatment on the surface (shown bright yellow in the HTML color version). The CML particles are the same kind as the ones used in the single particle concentration. The mobility of the CML particles in DI water was roughly estimated at about 1 μm s^{-1} V^{-1} cm, while that of the polystyrene particles was close to zero. When an electric field (approximately 3.3 V mm^{-1}) is generated in the water droplet by applying a voltage between the two open contacts on the top plate, the CML particles are electrophoretically migrated to the left (anode) while the polystyrene particles overall drift to the right (Fig. 8(b)).

Meanwhile, a vortex, similar to the one observed during the particle concentration in the previous section, forms in the middle of the mother droplet (Fig. 8(c)). Vortex or circulation generation in a droplet is a relatively unknown phenomenon. It seems to occur in a wide range of configurations showing similar patterns, more likely in a confined space such as droplet configurations. During the initial period of about 30 s after an electric field is applied, the strongly charged CML particles are attracted to the anode as expected, while uncharged polystyrene particles seemingly *drift* to the cathode. Then, a vortex starts to form in the middle of the droplet, in which the two types of particles are gathered and circulated with respect to the circulating axis pointing in the lateral direction. As time goes by, this circulating axis becomes distorted showing wavy patterns (Fig. 8(c)). Three-dimensional instability seems to be developed. Apparently, this phenomenon would lower the separation efficiency. The particles in the circulating region remain mixed, not separated even when a higher electric field is applied.

Nevertheless, overall the two types of particles are separated into two opposite regions inside the droplet, *i.e.*, the CML particles on the left and the polystyrene particles on the right (Fig. 8(c)). The subsequent splitting step by EWOD actuations (Fig. 8(d)) makes the two regions physically divided into two daughter droplets, completing the separation and extraction

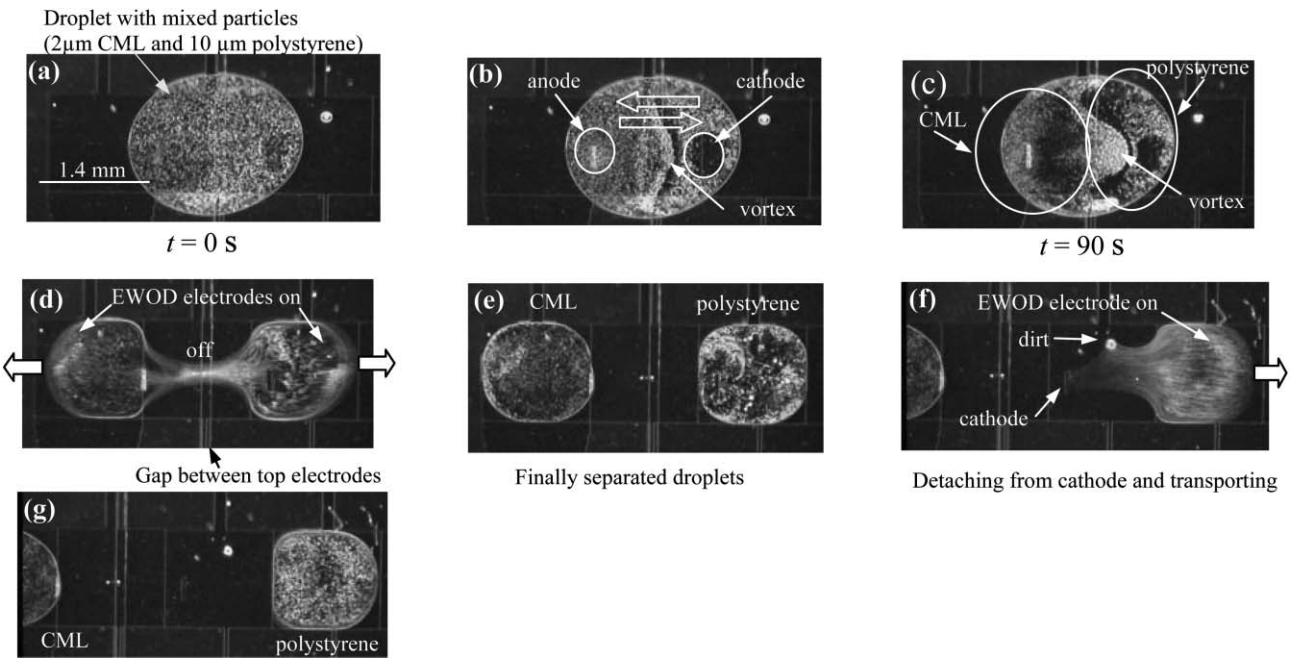

Fig. 8 Sequential pictures of particle separation viewed through the top glass cover: (a) Initially CML particles (negatively charged, shown dark yellow in the HTML color version) and polystyrene particles (no charge treatment, shown bright yellow in the HTML color version) are mixed uniformly in a mother droplet; (b) electrophoresis on. The CML particles move to the anode while the polystyrene particles move to the right. Note that the vortex starts to form in the middle of the droplet; (c) vortex line is distorted into a wavy pattern; (d) the mother droplet is split into two daughter droplets by EWOD actuation; (e) the CML particles are concentrated in the left droplet while the polystyrene particles in the right; (f) the right droplet is successfully transported away from the separation site. Note that the tail of the droplet is pinned on the cathode surface and the dirt for a moment; (g) completion of the whole separation process.

procedures. The left and right EWOD driving electrodes at the two opposite ends of the droplet are activated at V_E = 60 V_{AC} and 10 kHz with the middle electrode off such that the droplet starts to elongate and the middle of the droplet contracts. The split process itself is completed within 1/15 s. Finally, the CML particles are more concentrated in the left daughter droplet than the right, and vice versa for the polystyrene particles (Fig. 8(e)). Afterwards, freeing the right droplet from the separation site is successfully accomplished (Fig. 8(f)) despite the momentary appearance of a liquid tail pinned on the hydrophilic cathode surface. In this figure, dirt on the surface is shown to cause additional pinning.

4.2.2 Quantification of particle separation. The quantification of binary particle separation was carried out at two different cut-off times ($t_{cut\text{-}off}$ = 60 s and 180 s). Here, 180 s was observed long enough for the full development of a vortex. In these two different cut-off times, distinct separation behaviours occur, as shown in Fig. 9 and Tables 2 and 3. At $t_{cut\text{-}off}$ = 60 s, as shown in Table 2, the concentration of CML particles C_{CML} for the left daughter droplet is significantly larger than that for the right, and the concentration of polystyrene particles C_{Pol} for the right daughter droplet is larger than that for the left. A great number of particles of each type are separated into each split daughter droplet. As a result, the concentration ratios of the CML-to-polystyrene particles C_{CML}/C_{Pol} are 21.9 and 5.3 in the left and right droplet, respectively. The ratio before separation was initially 10.6. Also, percentiles of separated particles for each droplet are shown in parentheses in Table 2. 66% of the total CML particles are separated into the left droplet, while 68% of the total polystyrene particles are separated in the right droplet.

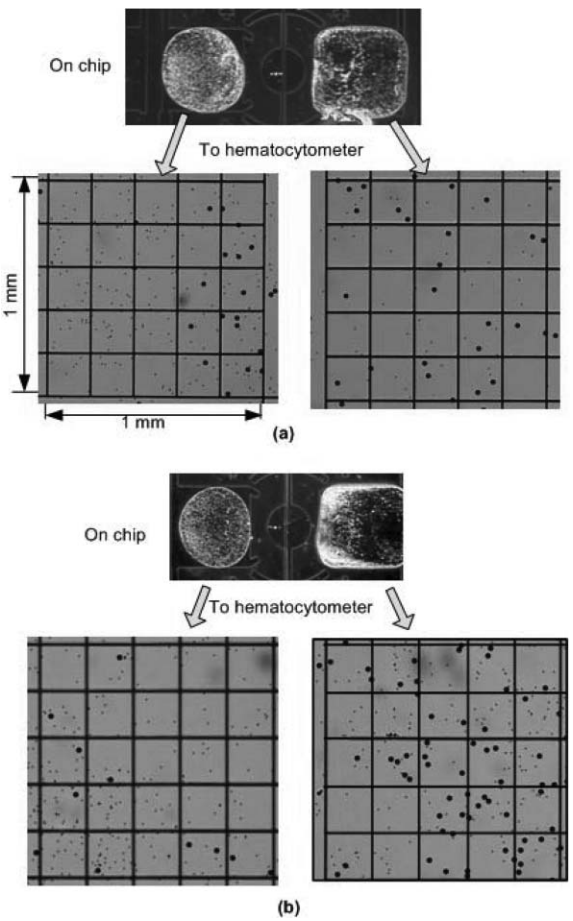

Fig. 9 On-chip images and their corresponding hematocytometer images of particle separation at (a) $t_{cut\text{-}off}$ = 60 s and (b) 180 s. Before separation, the mother droplet had a uniform mixture of 2 μm CML and 10 μm polystyrene particles.

Table 2 Concentration in each droplet at $t_{cut\text{-}off}$ = 60 s (the numbers in parentheses represent the percentile to the total number of particles of each type)

	Before separation	After separation	
		Left droplet	Right droplet
Concentration of CML, C_{CML}/number of particles μl^{-1}	30 158	47 938 (66%)	17 532 (34%)
Concentration of polystyrene, C_{Pol}/number of particles μl^{-1}	2853	2190 (32%)	3321 (68%)
C_{CML}/C_{Pol}	10.6	21.9	5.3

[a] Volumes of left and right droplets are 0.18 and 0.25 μl, respectively.

At $t_{cut\text{-}off}$ = 180 s, the vortex near the middle of the mother droplet was fully developed. This results in changes in C_{CML} and C_{Pol}, as shown in Table 3. Compared to the concentrations at $t_{cut\text{-}off}$ = 60 s, C_{CML} decreases in the left droplet and increases in the right, deteriorating the separation efficiency. Even the percentage of CML particles to the total particles in the left droplet is slightly smaller than that in the right droplet. On the contrary, the separation efficiency for polystyrene particles is enhanced. This change is closely related to the vortex formation. The vortex brings a strong circulating flow in the middle of the droplet, which contains a significant number of CML as well as polystyrene particles. Depending on whether this vortex flow region belongs to the left or right daughter droplet after the mother droplet is split, significant concentration changes occur as a result. This concentration is very sensitive to which daughter droplet takes the vortex region in the process of splitting. In this experiment, it is speculated that the right daughter droplet took a significant portion of the vortex flow, considering the volume ratio of the right-to-left droplets for the case of $t_{cut\text{-}off}$ = 180 s was greater

Table 3 Concentration in each droplet at $t_{cut\text{-}off}$ = 180 s

	Before separation	After separation	
		Left droplet	Right droplet
Concentration of CML, C_{CML}/number of particles μl^{-1}	31 234	38 418 (48%)	26 560 (52%)
Concentration of polystyrene, C_{Pol}/number of particles μl^{-1}	2957	722 (9%)	4416 (91%)
C_{CML}/C_{Pol}	10.6	53.2	6.0

[a] Volumes of left and right droplets are 0.16 and 0.25 μl, respectively.

than that for the case of $t_{cut\text{-}off}$ = 60 s. Consequently, the final concentration ratios C_{CML}/C_{Pol} are 53.2 and 6.0 in the left and right droplets, respectively. Note that, although C_{CML}/C_{Pol} for the left droplet is much higher than that for $t_{cut\text{-}off}$ = 60 s, C_{CML} itself and its corresponding particle percentage for the left droplet are lower than those for the case of $t_{cut\text{-}off}$ = 60 s. This is due mainly to the low concentration of the polystyrene particle in the left droplet.

5. Discussions

The series of experimental results along with efficiency quantifications prove the concept of the concentration and separation schemes. Although the current device implemented electrophoretic separation of particles, the described scheme may adopt any of many other particle separation principles such as dielectrophoresis,[42] magnetophoresis, ultrasonic standing waves, and so on, which are currently under exploration.

At the present stage, the concentration efficiency of a single type of particle is promising, showing that about 83% of total particles are concentrated into a split droplet having ~50% volume of the mother droplet, *i.e.*, ~70% increase in the concentration. The separation of two different types of particles is encouraging although the efficiency was lower than that of the concentration. When the droplet is split before the vortex is fully developed, about 66% of the total CML particles and 68% of the total polystyrene particles are separated into the respective daughter droplets. However, once the vortex is fully developed, the separation becomes less controllable. For higher separation and concentration efficiencies, it is necessary to understand and suppress vortex or circulation generation. Note that, in any case, the efficiency may be improved by repeating the concentration or separation procedure after collecting the daughter droplets into a new large mother droplet.

What is responsible for this vortex generation? Similar circulating flows under an electric field can be found in the literature. Green *et al.*[43,44] reported circulating flow patterns induced by an electrothermal effect. Joule heating or light illumination generated temperature gradients in the fluid, affecting gradients in the fluid permittivity and conductivity which induced the driving force of the circulating flow patterns. To examine this electrothermal effect in the present configuration, the electric field was kept off for 5 min for sufficient cooling once vortex flow pattern was developed, and was switched back on again. However, the vortex flow pattern resumed shortly (in less than 2 s). Considering that it generally takes at least 10 s for the initial vortex build-up, the result suggests that the electrothermal effect is not responsible for this vortex formation. Circulating flow patterns were also reported in AC electro-osmotic flows[45] where an AC field was used. However, the applied electric field for electrophoresis is DC in the present configuration, not AC.

One of the possible scenarios is due to collision between two flows generated in the droplet: one is a particle-dragged flow and the other is a rebounded flow due to the fixed meniscus boundary. Under an electric field, the strongly charged particles (*i.e.*, CML particles) migrate and, at the same time, drag the surrounding fluid to the anode. The fluid and particles are therefore accumulated in the anode area. This accumulation generates a rebounded flow towards the region where the CML particles and their surrounding fluid were. The rebounded flow is in the opposite direction to the CML-dragged flow. Interestingly, the polystyrene particles seem to drift with the rebounded flow to the right side of the droplet since they are not significantly attracted by the electrostatic charge. After a certain time, there must be a competition between the dragged and rebounded flows due to their opposite directions, finally resulting in circulations in the middle of the droplet. In order to verify this scenario, however, more studies are required.

It is relevant to point out that, if the polystyrene particles are drifted on the rebounded flow, and not strongly attracted by the electric field, two different types of particles may be separated by the mobility difference (that is, they might not have to be necessarily in the opposite polarity to each other). This will be very useful since particles of the same polarity may be separated by the mobility difference in the droplet configuration. However, in order to assess this possibility clearly, a wide range of particle combinations need to be examined in the droplet configuration.

6. Conclusions

In this paper, we described a particle concentration and separation scheme for droplet-based digital microfluidic systems operated by the EWOD principle. The concept was proven experimentally using microfabricated testing devices. The separation scheme of two different types of particles consists of three steps: (1) isolate each type of particle by electrophoresis into a designated region inside a mother droplet, (2) physically split the mother droplet into two daughter droplets by EWOD actuation so that the isolated particles of each type are concentrated into each daughter droplet, and (3) transport the daughter droplets by EWOD to other locations for follow-up microfluidic operations. Similarly, by applying the separation scheme to a droplet containing only one type of particles, the particle can be concentrated into a daughter droplet.

Successful concentration was experimentally demonstrated using negatively charged CML particles. The off-chip particle counting method showed that 83% of the total particles are concentrated into a half-size daughter droplet, *i.e.*, ~70% increase in concentration. Also, binary separation was successfully demonstrated using two different types of particles: negatively charged CML particles and no-charge-treated polystyrene particles. When the droplet is split before a vortex is fully developed, 66% of the total CML particles are separated into one daughter droplet and 68% of the total polystyrene particles are separated in the other daughter. In both concentration and separation cases, in the meantime, vortex formation was observed in the middle of the droplet, lowering the concentration and separation efficiency. For higher efficiency and more precise control, focused studies on a vortex phenomenon are needed. Although the overall efficiency at the current stage is not high enough for practical use, the present method will introduce a new class of concentration and separation concept and its improved design may constitute

a fundamental fluidic unit for emerging digital microfluidics and widen its application spectrum.

Acknowledgements

This work was supported by the NSF Engineering Microsystems: "XYZ on a chip" Program, the Defense Advanced Research Projects Agency (DARPA) BioFlips Program and the HSARPA (Homeland Security Advanced Research Projects Agency) SBIR project through the Core MicroSolutions Inc.

References

1 C. H. Ahn, J.-W. Choi, G. Beaucage, J. H. Nevin, J.-B. Lee, A. Puntambekar and J. Y. Lee, Disposable smart lab on a chip for point-of-care clinical diagnostics, *Proc. IEEE*, 2004, **92**, 154.
2 A. W. Chow, Lab-on-a-chip: Opportunities for chemical engineering, *AIChE J.*, 2002, **48**, 1590.
3 G. Ehrenman, Shrinking the lab down to size, *Mech. Eng.*, 2004, **126**, 26.
4 R. Ehrnstrom, Miniaturization and integration: challenges and breakthroughs in microfluidics, *Lab Chip*, 2002, **2**, 26N.
5 J. G. E. Gardeniers and A. v. d. Berg, Lab-on-a-chip systems for biomedical and environmental monitoring, *Ann. Bioanal. Chem.*, 2004, **378**, 1700.
6 A. R. Kopf-Sill, Successes and challenge of lab-on-a-chip, *Lab Chip*, 2002, **2**, 42N.
7 A. Manz, N. Grabber and H. M. Widmar, Miniaturized total analysis systems: a novel concept for chemical sensing, *Sens. Actuators, B*, 1990, **1**, 244.
8 J. Lee, H. Moon, J. Fowler, C.-J. Kim and T. Schoellhammer, Addressable micro liquid handling by electric control of surface tension, *Proc. IEEE Conf. MEMS*, 2001, 499.
9 J. Lee, H. Moon, J. Fowler, T. Schoellhammer and C.-J. Kim, Electrowetting and electrowetting-on-dielectric for microscale liquid handling, *Sens. Actuators, A*, 2002, **95**, 259–268.
10 M. G. Pollack, R. B. Fair and A. D. Shenderov, Electrowetting-based actuation of liquid droplets for microfluidic applications, *Appl. Phys. Lett.*, 2000, **77**, 1725.
11 M. G. Pollack, A. D. Shenderov and R. B. Fair, Electrowetting-based actuation of droplets for integrated microfluidics, *Lab Chip*, 2002, **2**, 96.
12 S. K. Cho, S.-K. Fan, H. Moon and C.-J. Kim, Towards digital microfluidic circuits: creating, transporting, cutting and merging liquid droplets by electrowetting-based actuation, *Proc. IEEE Conf. MEMS*, 2002, 32.
13 S. K. Cho, H. Moon and C.-J. Kim, Creating, transporting, cutting, and merging liquid droplets by electrowetting-based actuation for digital microfluidic circuits, *J. Microelectromech. Syst.*, 2003, **12**, 70–80.
14 M. Washizu, Electrostatic actuation of liquid droplets for microreactor application, *IEEE Trans. Ind. Appl.*, 1998, **34**, 732.
15 T. B. Jones, M. Gunji, M. Washizu and M. J. Feldman, Dielectrophoretic liquid actuation and nanodroplet formation, *J. Appl. Phys.*, 2001, **89**, 1441.
16 J. A. Schwartz, J. V. Vykoukal and P. R. C. Gascyne, Droplet-based chemistry on a programmable micro-chip, *Lab Chip*, 2004, **4**, 11.
17 T. Tanigichi, T. Torii and T. Higuchi, Chemical reactions in microdroplets by electrostatic manipulation of droplets in liquid media, *Lab Chip*, 2002, **2**, 19.
18 O. D. Velev, B. G. Prevo and K. H. Bhatt, On-chip manipulation of free droplets, *Nature*, 2003, **426**, 515.
19 A. A. Darhuber, J. P. Valentino, S. M. Troian and S. Wagner, Thermocapillary actuation of droplets using microheater arrays, *J. Microelectromech. Syst.*, 2003, **12**, 873–879.
20 T. K. Jun and C.-J. Kim, Valveless pumping using traversing vapor bubbles in microchannels, *J. Appl. Phys.*, 1998, **83**, 5658.
21 T. A. Sammarco and M. A. Burns, Thermocapillary pumping of discrete drops in microfabricated analysis devices, *AIChE J.*, 1999, **45**, 350.
22 C.-J. Kim, "Micromachines driven by surface tension, 30th AIAA Fluid Dynamics Conference, 1999, **1**, (AIAA 99–3800).
23 J. Lee and C.-J. Kim, Surface tension driven microactuation based on continuous electrowetting (CEW), *J. Microelectromech. Syst.*, 2000, **9**, 171.
24 H. Matsumoto and J. E. Colgate, Preliminary investigation of micropumping based on electrical control of interfacial tension, *Proc. IEEE Workshop MEMS*, 1990, 105.
25 F. Mugele and J.-C. Baret, Electrowetting: from basics to applications, *J. Phys.: Condens. Matter*, 2005, **17**, R705–R774.
26 B. Berge, Electrocapillarity and wetting of insulator films by water, *C. R. Acad. Sci., Ser. II*, 1993, **317**, 157.
27 H. Moon, S. K. Cho, R. L. Garrell and C.-J. Kim, Low voltage electrowetting-on-dielectric, *J. Appl. Phys.*, 2002, **92**, 4080.
28 J. Fowler, H. Moon and C.-J. Kim, Enhancement of mixing by droplet based microfluidics, *Proc. IEEE Conf. MEMS*, 2002, 97.
29 P. Paik, V. K. Pamula and R. B. Fair, Rapid droplet mixers for digital microfluidic systems, *Lab Chip*, 2003, **3**, 253.
30 S.-K. Fan, C. Hashi and C.-J. Kim, Manipulation of multiple droplets on $N \times M$ grid by cross-reference EWOD driving scheme and pressure-contact packaging, *Proc. IEEE Conf. MEMS*, 2003, 694.
31 J. Gong and C.-J. Kim, Two-Dimensional Digital Microfluidic System by Multi-Layer Printed Circuit Board, Proc. IEEE MEMS 2005, Miami, Florida, 2005, pp. 544–547.
32 J. Gong, S.-K. Fan and C.-J. Kim, Portable digital microfluidics platform with active but disposable lab-on-chip, *Proc. IEEE Conf. MEMS*, 2004, 355.
33 V. Srinivasan, V. K. Pamula and R. B. Fair, Droplet-based microfluidics lab-on-a-chip for glucose detection, *Anal. Chim. Acta*, 2004, **507**, 145.
34 A. R. Wheeler, H. Moon, C.-J. Kim, J. A. Loo and R. L. Garell, Electrowetting-based microfluidics for analysis of peptides and proteins by matrix-assisted laser desorption/ionization mass spectrometry, *Anal. Chem.*, 2004, **76**, 4833–4838.
35 A. R. Wheeler, H. Moon, C. A. Bird, R. R. O. Loo, C.-J. Kim, J. A. Loo and R. L. Garrell, Digital microfluidics with in-line sample purification for proteomics analyses with MALDI-MS, *Anal. Chem.*, 2005, **77**, 534–540.
36 H. Moon, A. R. Wheeler, R. L. Garrell, J. A. Loo and C.-J. Kim, On-chip sample preparation by electrowetting-on-dielectric digital microfluidics for matrix assisted laser desorption/ionization mass spectrometry, *Proc. IEEE Conf. MEMS*, 2005, 859.
37 Y. Zhao and S. K. Cho, A micro particle sampler using electrowetting-actuated droplet sweeping, the 13th International Conference on Solid-State Sensors, Actuators, and Microsystems (Transducers 2005), Seoul, Korea, 2005, pp. 129–134.
38 Y. Zhao and S. K. Cho, Microparticle sampling by electrowetting-actuated droplet sweeping, *Lab Chip*, 2006, **6**, 137–144.
39 H. Morgan and N. G. Green, AC Electrokinetics, Colloids and Nanoparticles, Research Studies Press Ltd., Baldock, Hertfordshire, UK, 2003.
40 S. K. Cho and C.-J. Kim, Particle separation and concentration control for digital microfluidic systems, *Proc. IEEE Conf. MEMS*, 2003, 686.
41 C. C. Cho, R. M. Wallace and L. A. Filessesler, Patterning and etching of amorphous Teflon films, *J. Electron. Mater.*, 1994, **23**, 827.
42 Y. Zhao, U.-C. Yi and S. K. Cho, In-droplet particle separation by travelling wave dielectrophoresis (twDEP) and EWOD, Solid-State Sensors, Actuators, and Microsystems Workshop, Hilton Head Island, South Carolina, 2006, pp. 181–184.
43 N. G. Green, A. Ramos, A. Gonzalez, A. Castellanos and H. Morgan, Electric field induced fluid flow on microelectrodes: the effect of illumination, *J. Phys. D*, 2000, **33**, L13.
44 N. G. Green, A. Ramos, A. Gonzalez, A. Castellanos and H. Morgan, Electrothermally induced fluid flow on microelectrodes, *J. Electrost.*, 2001, **53**, 71.
45 N. G. Green, A. Ramos, A. Gonzalez, H. Morgan and A. Castellanos, Fluid flow induced by nonuniform ac electric fields in electrolytes on microelectrodes. I. Experimental measurements, *Phys. Rev. E*, 2000, **61**, 4011.

